Studies of Chain Conformation in Triblock Oligomers and Microblock Copolymers of Ethylene and Ethylene Oxide

Yaqiang Ding and John F. Rabolt*

Department of Materials Science and Engineering, University of Delaware, DuPont Laboratories, Newark, Delaware 19716

Y. Chen, Kirk L. Olson, and Gregory L. Baker

Department of Chemistry and Center for Fundamental Materials Research, Michigan State University, East Lansing, Michigan 48824

Received August 22, 2001; Revised Manuscript Received February 28, 2002

ABSTRACT: The conformation of ethylene oxide segments has been found to vary when they are incorporated into triblock oligomers $[H(CH_2)_m(CH_2CH_2O)_n(CH_2)_mH]$ or microblock copolymers $[-(CH_2)_m-(CH_2CH_2O)_n-]_x$ of ethylene (E) and ethylene oxide (EO) depending on the relative length (m vs n) of the sequences. Raman spectroscopy, wide-angle X-ray diffraction, and thermal analysis have been used to investigate these conformational variations. Since both segments crystallize, we have found a profound influence of intermolecular interactions on determining the conformation of the EO segment. In the regime where $n < 7$ ($m = 12-20$), the EO segment is found in the planar zigzag conformation similar to that observed in oriented poly(ethylene oxide) (PEO) held under tension. When $n > 7$ ($m = 12-20$), the EO segments are found to crystallize in the 7/2 helical conformation similar to that found in PEO. In the case where $n = 7$ ($m = 12-20$), both the helical and planar zigzag forms of EO are found depending on the thermal and solution processing history. The helical form can be induced by melt-quenching, but annealing at room temperature for several days produces a gradual return to the planar conformation. A conformational transition caused by solvents also occurs and will be discussed.

Introduction

Molecular architecture plays an important role in determining structure−property relationships in advanced materials. Unique diblock and triblock copolymer architectures and how phase separation in these advanced materials can create unique morphologies have been the subject of intense investigations over the past two decades.[1] The microstructure that results, after heating above the glass transition temperature, T_g, of the multiple component blocks, is primarily driven by competing inter- and intramolecular interactions. These interactions lead to microphase separation, which gives rise to different morphologies such as spheres, rods, and lamella depending on the relative molecular weight of the component blocks.[2] There are a number of potentially interesting applications for diblock and triblock copolymers such as food additives, stratified layer optical waveguides, and electronic components.

Most studies thus far have focused on amorphous−amorphous diblocks (e.g., poly(styrene) (PS)−poly(methyl methacrylate) (PMMA)) in the melt or solid phase, but there are also some reports on diblocks and triblocks in solution.[3−5] Knowledge obtained from these studies has provided insights into the use of diblock copolymers as compatibilizers, surface modifiers, and mechanical property enhancers. Although numerous investigations into the properties of diblock and triblock copolymer systems have been published, the primary architecture that has been studied has been the one where the component blocks are amorphous. Only recently has there been reports of amorphous−crystalline and amorphous−liquid crystalline diblock[6] copolymers that have been shown to exhibit unique ordering characteristics. The highly ordered structures that result show considerable promise as optical components if defects can be minimized and optical clarity improved. So far, only minimal work on crystalline−crystalline diblock and triblock copolymers have appeared in the literature. In these studies, a series of short-chain semifluorinated n-alkanes, $F(CF_2)_n(CH_2)_mH$ ($n = 6-12$, $m = 1-20$), were investigated[7−9] in both the melt and solid state. Depending on the relative length of fluorocarbon vs hydrocarbon segments in the chain, different crystalline packing arrangements were observed. As a result of studies on triblock copolymers of this same family in which a hydrocarbon segment formed the center block, it has been observed that a conformational perturbation of the planar hydrocarbon block by the helical fluorocarbon end blocks occurs. The exact nature of the conformational change was not specifically determined, but spectroscopic evidence and thermal analysis indicated that the perturbed conformation was, in fact, ordered and that it was incorporated into the crystal lattice upon crystallization. This raised an interesting fundamental question about the effects of the backbone conformation of one block on an adjacent block of different chemical architecture in crystalline−crystalline triblock and microblock copolymers. When semifluorinated microblock copolymers were first reported in the literature,[10] it became clear that in small-angle X-ray diffraction measurements of $[-(CF_2)_n(CH_2)_6-]_m$, $n = 4, 6$, the layer line corresponding to the repeat distance along the polymer chain axis observed was too small to accommodate the hydrocarbon segment in an extended conformation, hence suggesting that the hydrocarbon segment either was tilted or adopted a nonplanar conformation.

* Corresponding author.

10.1021/ma011511o CCC: $22.00
Published on Web 04/16/2002

In the current study, we will investigate whether crystallization-induced conformational changes occur in any of the component blocks of crystalline−crystalline triblock E−EO oligomers and microblock copolymers. Unlike crystallization in a homopolymer where the polymer backbone usually adopts a single ordered conformation as it packs into a lattice, in crystalline−crystalline microblock copolymers there are a number of possible structures that can result. This could lead to the "templating" of the crystal motif by one of the blocks, but this will depend on the relative lengths of the blocks, the thermodynamic compatibility of the blocks, and their relative flexibility/rigidity. The latter could lead to cocrystallization of the multiple blocks with the resulting constrained geometry of the "hybrid" lattice leading to conformational change of one (or both) of the component blocks in order to accommodate the new intermolecular environment.

There is general interest in the chemical architecture of ethlylene−ethylene oxide block oligomers, partly because the chemical simplicity of their structures and because there has been many studies[11−17] on the individual homopolymers (PE and PEO). By appending hydrophilic blocks to hydrophobic blocks, a significant number of scientific and technological applications could result. Another motivation for choosing the ethlylene−ethylene oxide system is that it will be possible to utilize knowledge obtained from model diblock and triblock copolymers to design and synthesize the corresponding microblock copolymers, $[-(CH_2)_m-(CH_2CH_2O)_n-]_x$. Hence, the results of this study should provide a correlation between physical properties (e.g., melting point, mechanical properties) and n/m. In this way, we could establish a set of molecular design principles that would allow prediction of other properties of the microblock copolymers that could be accomplished by varying m and n.

In this paper, we will investigate a series of triblocks with the architecture of $H(CH_2)_{14}(CH_2CH_2O)_n(CH_2)_{14}H$ by varying n from 3 to 14 and a series of microblock copolymers $[-(CH_2)_{20}-(CH_2CH_2O)_n-]_x$ by varying n from 7 to 14. A comparison of the spectroscopic behavior of the individual triblock oligomers and microblock copolymers against other samples in the series is presented while other factors that could induce conformational change in triblocks and microblock copolymers, such as mechanical stretching, thermal history, and solvent, are also investigated.

Experimental Section

Instrumentation. The Raman instrumentation used consisted of a HoloSpec f/1.8iVPT system (holographic imaging spectrograph) manufactured by Kaiser Optical Systems, Inc., a SDL-8530 wavelength-stabilized high-power laser, a detector controller from Princeton Instruments Inc., and a HoloLab series 5000 Olympus microscope interfaced to the Raman system by Kaiser optical systems, Inc.

Raman data were obtained using 785 nm laser excitation. The typical number of scans taken for each sample was six with each scan being 45 s in duration. A 10× magnification was used when spectra were recorded with the Raman microscope. Dark Subtract and Cosmetic Ray filters were also employed. Laser power was adjusted to maximum (approximately 70 mW) for most samples to increase power input and S/N ratio of the spectra obtained.

Sample Preparation. The E−EO−E triblock oligomers were prepared by the reaction of alkyl bromides with the disodium salt of the desired ethylene oxide oligomer. The ethylene glycol oligomers were synthesized by an iterative process that ensured that they are of exact length rather than a distribution of chain lengths. E−EO−E compounds that are liquids at room temperature were purified by distillation; all other compounds were crystallized from acetone or methanol. Complete synthetic details and physical data appear elsewhere.[18] $(E-EO)_n$ microblock copolymers were synthesized by the ADMET polymerization of α,ϖ-dienes that contain an oligoethylene oxide core using Schrock's molybdenum catalyst. The monomers were prepared using the same procedure as used for the E−EO−E oligomers, except that the alkyl bromides were replaced by ω-alkenyl bromides. The monomers were purified over sodium mirrors and stored in a drybox. The polymerizations were carried out in the absence of air and typically yielded polymers with $M_n > 50\,000$ g/mol. The polymers were purified by precipitation from heptane and were stored in a drybox prior to use.[19]

Numerous triblocks of the form $H(CH_2)_m(CH_2CH_2O)_n(CH_2)_mH$ were prepared[16] and are referred to according to the notation, $m-n-m$. For example, 14−8−14 is the notation for $H(CH_2)_{14}(CH_2CH_2O)_8(CH_2)_{14}H$. Additional microblock copolymers of the form $[-(CH_2)_m(CH_2CH_2O)_n-]_x$ were also prepared and referred to according to the notation P(m,n). For example, P(20,14) is the notation for $[-(CH_2)_{20}(CH_2CH_2O)_{14}-]_x$.

The following triblock oligomers and microblock copolymers were synthesized at Michigan State University:[16]

14−3−14, 14−5−14, 14−7−14, 14−8−14, 14−10−14, 14−14−14

16−3−16, 16−5−16, 16−7−16, 16−8−16

P(20,7), $M_W = 57\,300$; P(20,8), $M_W = 90\,300$

P(20,10), $M_W = 76\,900$; P(20,14), $M_W = 103\,500$

The PEO Polyox WSR n-750 (Union Carbide Chemicals Co., MW = 300 000, MP = 65 ± 2 °C) coagulant powder, used to prepare the thin film for the stretching experiment, was provided by Union Carbide Chemical Co.

Melt-pressed PEO films were cold-drawn at room temperature to about 8 times their original length by a homemade extension apparatus. During the data acquisition process, these uniaxially oriented specimens were kept under tension, and the laser focused on only the most extended crystalline region.

Powder samples, pressed to increase their density and hence optimize their scattering volume, were investigated in an aluminum DSC pan. Liquid samples were studied below their freezing points by bathing the sample in gaseous nitrogen circulated through a liquid nitrogen bath. An enclosure holding the sample was purged with N_2 to remove the moisture so that no frost was accumulated on the glass capillary holding the sample. Spectra of colored polymer samples that contained small amounts of fluorescing impurities were collected after being photobleached for 5−7 h to reduce the fluorescence.

Results and Discussion

Helix-to-Planar Zigzag Conformational Transition of PEO by Mechanical Stretching. Raman spectra of drawn PEO were recorded consecutively while increasing the draw ratio, and a significant change in the spectrum was observed as shown in Figure 1. The transition from helical to planar zigzag conformation was observed to be fairly abrupt once a critical draw ratio was reached. Tashiro et al.[11] found that the critical value for the applied stress that could induce the transition from helical to planar zigzag chains was 9.7×10^{11} dyn/cm.[4] It should be noted that once the fiber is relaxed and no strain is applied to the PEO fiber, the new planar zigzag peaks at 1495, 1041, and 1151 cm^{-1} disappear immediately, indicating that the transition process from helical to planar zigzag chains is reversible.

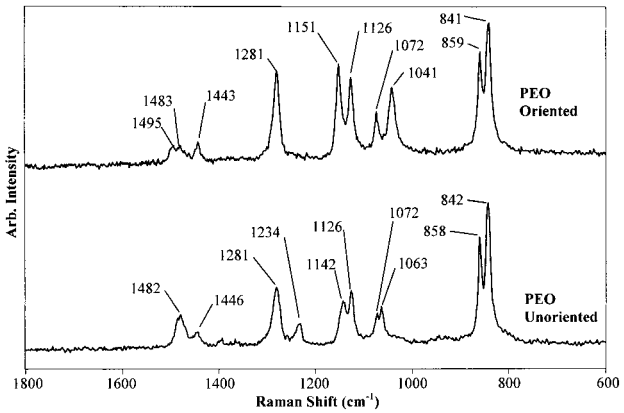

Figure 1. Helical-to-planar zigzag transition by mechanically stretching poly(ethylene oxide). Unoriented PEO film has a helical conformation (bottom). In the Raman spectrum of a highly drawn PEO film (top), three new bands characteristic of a planar zigzag conformation appear at 1495, 1041, and 1151 cm^{-1}.

Hence, it is clear from the reversibility of this process that the planar zigzag conformation obtained under tension is metastable and may change back to helical conformation once the stress is released.

Infrared studies and X-ray diffraction measurements[12] have shown that the molecular conformation of poly(ethylene oxide) is a 7/2 helix. When the PEO sample is highly drawn and held under stress, the original conformation is distorted. Raman measurements (Figure 1) show that a repeatedly stretched sample held under tension gives us three new bands at 1495 cm^{-1} (CH_2 bending), 1041 cm^{-1} (CH_2 rocking), and 1151 cm^{-1} (CC stretching). The two new peaks at 1151 and 1041 cm^{-1} are reasonably strong while that at 1495 cm^{-1} is of medium intensity. X-ray studies[13] indicated that this extended crystalline conformation has a fiber period of 7.12 Å with the bond lengths of 1.54 Å (C−C) and 1.43 Å (C−O) with a CCO bond angle of 109° 28′. Calculations showed that the planar zigzag PEO has a fiber period of 7.18 Å, which corresponds to the experimental value of 7.12 Å. At the stress-induced phase transition from helix to planar zigzag conformation, the rotation about C−O bonds causes a change in the conformational sequences of the ethylene oxide from TTG (7/2 helix) to TTT (planar), where T and G denote trans and gauche, respectively. Calculations also show that the length per monomeric unit along the draw direction increases from 2.78 to 3.56 Å during the stretching process.

It is also observed that oriented PEO is actually a blend of both planar-zigzag and helical conformations which is expected because of the way it was mechanically stretched. While some molecules with planar zigzag conformation are obtained, the helical form is not completely eliminated due to the limitations of the drawing techniques and the presence of amorphous PEO. In the drawing direction, the helical chains would all be converted to planar zigzag ones if an extended chain morphology was first produced. However, this is not the case, and in fact, the stress during draw is not uniformly distributed on all crystalline regions. Thus, helical chains still exist, and their characteristic $-CH_2-$ bending peak still appears in the Raman spectrum at 1483 cm^{-1}, with an intensity comparable to the 1495 cm^{-1} band attributable to the newly created planar zigzag chains. The two strong peaks at 859 and 841 cm^{-1} are also of some interest and are believed to be the result of the ordered helical conformation.[14] In Figure 1, these peaks are still reasonably strong when the critical stress level to induce helical/planar-zigzag transition has been reached. This observation also suggests that the helical chains could not be eliminated but only reduced by mechanical stretching. (However, as we will see soon, by controlling molecular architecture, a 100% conversion ratio from helical to planar zigzag chains can be achieved.) Note that the relative intensity of the peaks at both 859 and 841 cm^{-1} have been reduced during the stretching process, which suggests that the number of helical chains does decrease.

Table 1 lists the Raman bands in the region 600−1800 cm^{-1} for oriented and isotropic PEO. Those bands that appeared during the stretching process are associated with helical/planar zigzag transition. Note that three new bands appeared at 1495, 1041, and 1151 cm^{-1} and another three bands at 1063, 1142, and 1234 cm^{-1} disappeared completely after stretching. As discussed previously, other bands at 841, 858, and 1482 cm^{-1} decrease in intensity. Peak assignments in Tables 1−3 are based on Yoshihara et al.[15] This assignment will be discussed further in the section on triblock oligomers.

Helical−Planar Zigzag Conformational Transition in $E_m-(EO)_n-E_m$ Triblock Oligomers. Ethylene and ethylene oxide homopolymers have a significantly different conformation in their crystalline state due to the flexibility of the C−O bond and the different intermolecular interactions in the crystal. Ethylene segments adopt a planar zigzag conformation when they crystallize, while the ethylene oxide segment tends to be helical as discussed previously.

Triblocks with an A−B−A architecture,[16] where A = $H(CH_2)_m$ and B = $(CH_2CH_2O)_n$, have been investigated as a function of m vs n. The experimental data indicate that the $-(EO)_n-$ conformation can be controlled by manipulating its length relative to the length of the ethylene sequence. In the Raman spectra shown in Figure 2, new bands characteristic of the planar zigzag conformation appear at 1497, 1150, and 1044 cm^{-1} after the length, n, of the central $-(EO)_n-$ block in the triblock series of 14−n−14 is reduced to 7 or less. The disappearance of three bands at 861, 844, and 1231 cm^{-1} indicates that these three bands must be associated with helical conformation. As discussed earlier, the two bands at 861 and 844 cm^{-1} change in intensity during the mechanical stretching of PEO, but their absence in triblocks where the $-(EO)_n-$ sequence is equal to or shorter than 7 confirms their assignment to vibrations of the 7/2 helix. The same conformational transition was also observed with the 16−n−16 series for $n \leq 7$.

The planar zigzag $-(EO)_n-$ sequence in these triblocks with $n \leq 7$ is a consequence of the rotation about the C−O bonds under the constraints provided by the lattice packing dictated by the planar E blocks. Although the planar form of PEO obtained under tension is metastable, the planar zigzag conformation of short EO sequences in the triblock is clearly stable at room temperature.

As shown in Figure 2, there is an abrupt transition from planar zigzag to helix at $n \leq 7$ in the Raman spectra of the triblocks as indicated by the appearance of bands at 1481, 1231, and 840 cm^{-1}. Since the most stable conformation for PEO is a 7/2 helix, this suggests that a minimum length of 7 is required for the PEO core

Table 1. Raman Bands in the Region 600−1800 cm^{-1} for Oriented and Unoriented PEO[a]

oriented PEO Raman shift (cm^{-1})	unoriented PEO Raman shift (cm^{-1})	peak assignment	contribution	conformation
841 s	842 s	$r(CH_2)$	helical	tgt
859 s	858 s	$r(CH_2)$, $\nu_s(COC)$	helical	tgt
1041 m		$r(CH_2)$, $\nu_a(COC)$	planar zigzag	tgg
	1063 m	$r(CH_2)$, $\nu_s(COC)$		tgt, ttt
1072 w	1072 w	$r(CH_2)$, $\nu_s(COC)$		tgt
1126 m	1126 s	$\nu_s(COC)$		ttt, tgt
	1142 m	$\nu_a(COC)$	helical	t, g
1151 s			planar zigzag	ttt
	1234 w	$t(CH_2)$	helical	ttt, ttg, tgt
1281 s	1281 m	$t(CH_2)$		ttt, tgt
1443 w	1446 w	$\delta(CH_2)$		tgg, tgt
1483 w	1482 m	$\delta(CH_2)$	helical	tgt
1495 w			planar zigzag	ttt

[a] Band intensities: w (weak); m (medium); s (strong). Mode: r (rocking); t (torsion); ν(stretching); δ (bending). The assignment subscripts "a" and "s" stand for asymmetric and symmetric motions.

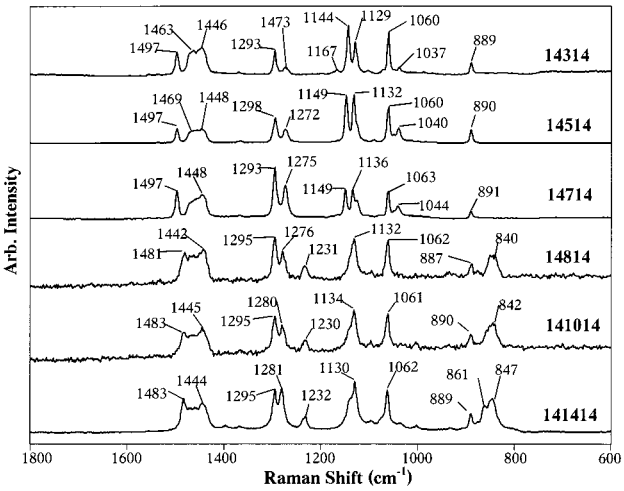

Figure 2. Helical−planar zigzag transition by manipulating the length of $(EO)_n$ in triblocks of the architecture $E_{14}-(EO)_n-E_{14}$. New bands characteristic of the planar zigzag conformation have appeared after a critical length of 7 has been reached as we reduce the length of central $-(EO)_n-$ block.

to be long enough to fit into one translational repeat unit of the helical conformation. The result suggests that, when E−EO triblocks (with $-(EO)_n-$ center block, $n \geq 8$) crystallize, the lattice packing of the ethylene segments is no longer favorable for the $-(EO)_n-$ core. Instead, the alkyl units in the ethylene segment adopt their normal planar zigzag conformation but tilt with respect to the EO core axis to accommodate the helical structure of the $-(EO)_n-$ core. Table 2 shows the peak assignments for both 14−3−14 and 14−14−14, which represent the triblock with an $-(EO)_n-$ length shorter than 7 (planar zigzag) and longer than 7 (helical), respectively.

Conformational Change of $(EO)_n$ in Alternating Microblock Copolymer Architectures. The previous sections detailed the conditions under which we could achieve helical-to-planar zigzag transition in both the PEO homopolymer and the triblock oligomers. Of significant interest is whether the conformational variations observed above are also observed in the microblock copolymers of the form $[-(CH_2)_m(CH_2CH_2O)_n-]_x$, designated as P($m$,$n$) in our notation.

The Raman spectra shown in Figure 3 have a significant similarity to that of low molecular weight counterparts shown in Figure 2. It is clear that two peaks characteristic of the planar zigzag conformation are observed at 1495 and 1148 cm^{-1}. However, unlike the 14−7−14, the spectra of P(20,7) does not show the planar zigzag band at 1044 cm^{-1} perhaps due to the shape of the background in that region.

Interesting enough, a *gradual* transition from planar-zigzag to helical conformation is observed for the P(20,n) microblock copolymers instead of the abrupt one observed in their triblock counterparts when the $-(EO)_n-$ length n is increased from 7 to 14. Unlike 14−7−14 and 14−8−14, the Raman spectra of P(20,7) and P(20,8) are very similar to each other as shown in Figure 3. The only difference between them is that in the spectra of P(20,8) the peak at 1495 cm^{-1} does not show up clearly, most likely due to an overlap with other peaks in the region. However, a peak characteristic of the planar zigzag conformation appears at 1148 cm^{-1} in P(20,8). On the basis of our previous observations in the triblocks, there should not be any bands which could be assigned to the planar zigzag conformation for P(20,8) since the length of the EO sequences is longer than 7, and therefore one might expect a 7/2 helical conformation. Since this is not the case, one can conclude that the transition from planar zigzag to helical with EO sequence length in the microblock copolymers is not as abrupt as in the case of the triblocks.

One plausible explanation is the folding of the long polymer molecules. It is well-known that polymer chains fold as they crystallize, and hence the lattice packing of the $-(EO)_n-$ segment could be influenced by the folding process. The folding region may cause conformational disorder that could give rise to bands that appear near those assigned to the helical conformation. Just like their triblock counterparts, the intensities of the two bands characteristic of a helical conformation (861 and 844 cm^{-1}) in those P(m,n) microblock copolymers are more intense for the polymer with longer EO sequences.

Table 3 shows the peak assignments for P(20, 7) and P(20,10), which represent the triblock with EO segments of a planar zigzag and helical conformation, respectively.

Conformational Transition of $-(EO)_7-$ in $E_{14}-(EO)_7-E_{14}$ Triblock by Melt-Quenching. Unlike other triblocks with a 14−n−14 molecular architecture, 14−7−14 may exhibit either a planar zigzag or helical conformation. This conformational change was observed during the melt-quenching of the powder 14−7−14 sample. The same transformation was not observed with other samples in the 14−n−14 series. In our experiment, the 14−7−14 powder was melted in a glass capillary and then quenched in liquid nitrogen. Comparison of the Raman spectrum taken after melt-

Table 2. Raman Bands in the Region 600−1800 cm^{-1} for Triblock 14−3−14 and 14−14−14[a]

14314 Raman shift (cm^{-1})	141414 Raman shift (cm^{-1})	peak assignment	contribution	conformation
	847 s	$r(CH_2)$	helical	tgt
	861 m	$r(CH_2)$, $\nu_s(COC)$	helical	tgt
889 w	889 w			
1037 w		$r(CH_2)$, $\nu_a(COC)$	planar zigzag	tgg
1060 s	1062 s	$r(CH_2)$, $\nu_s(COC)$		tgt, ttt
1129 s	1130 s	$\nu_s(COC)$		ttt, tgt
1144 s			planar zigzag	ttt
	1232 w	$t(CH_2)$	helical	ttt, ttg, tgt
1273 w	1281 s	$t(CH_2)$		ttt, tgt
1293 s	1295 s			
1446 s	1444 m	$\delta(CH_2)$		tgg, tgt
	1483 s	$\delta(CH_2)$	helical	tgt
1497 s			planar zigzag	ttt

[a] Band intensities: w (weak); m (medium); s (strong). Mode: r (rocking); t (torsion); ν (stretching); δ (bending). The assignment subscripts "a" and "s" stand for asymmetric and symmetric motions.

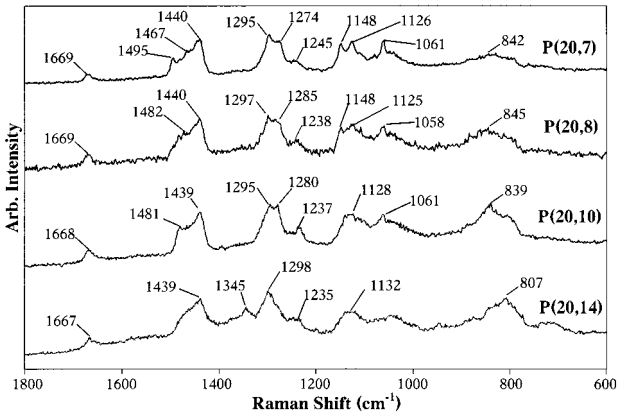

Figure 3. Helical−planar zigzag transition by manipulating the length of $(EO)_n$ in microblock copolymers of the architecture $[-E_{20}-(EO)_n-]_x$. Like their triblock counterparts, new bands characteristic of the planar zigzag conformation have appeared after a critical length of 7 has been reached as we reduce the length of central $(EO)_n$ block.

quenching (Figure 4) indicates that the conformation of the polymer chains has changed to a helical conformation.

Interesting enough, after melt-quenching, the helical conformation of the 14−7−14 chains is not stable, and eventually the conformation of the $-(EO)_7-$ block reverts back to the planar-zigzag form. This is also shown in Figure 4, where the Raman spectra of melt-quenched 14−7−14 obtained on day 0, day 2, day 4, and day 8 are shown. The slow process of transition from helical (day 0) to planar zigzag (day 8) conformation is clear. In fact, the spectrum of melt-quenched 14−7−14 on day 8 looks almost identical as that of powder 14−7−14 obtained before the heat treatment.

The time-lapse spectra clearly show that the helical band at 1483 cm^{-1}, which is present on day 0 and on day 2, shifts to 1497 cm^{-1} (planar zigzag) by day 4. The helical band at 1233 cm^{-1} also is present for more than 2 days and then disappears by day 4.

It is also interesting to note that the intensity of the helical doublet at 861 and 852 cm^{-1} gradually decreased with time and finally almost disappeared by day 8. The gradual transition from helical to planar zigzag could be explained by the fact that the conformation of the helical EO segment (of length $n = 7$) is metastable, converting into the planar zigzag form gradually as the sample anneals at room temperature.

This result suggests that the 14−7−14 prefers to stay in the planar zigzag form rather than the helical conformation under normal conditions. This is most likely related to the fact that seven ethylene oxide chemical repeating units are the shortest length which could be fit in a single translational repeat unit of a 7/2 helix, and therefore the $-(EO)_7-$ block has a tendency to adopt a planar conformation. The spatial arrangement and packing of this EO sequence in the lattice is planar zigzag instead of being helical due primarily to the templating of the crystal structure by the attached $H(CH_2)_{14}-$ blocks whose minimum-energy conformation is planar zigzag. This raises the interesting question of whether the $-(EO)_7-$ sequence in a 14−7 diblock oligomer would also be planar at room temperature. Although 14−7 was not studied specifically, Raman spectra of commercially available 12−8 and 12−6 were obtained at low temperatures (approximately −20 °C) and showed only the presence of the helical conformation as indicated by the appearance of bands at 1481, 1231, and 840 cm^{-1}. Thus, it appears that the templating of the crystal motif by $H(CH_2)_m-$ sequences occurs only if they are attached at both ends of the central $-(EO)_n-$ block, and this will lead to a planar zigzag conformation of the EO sequence provided $n \leq 7$.

Influence of Solvent on the Conformation of Ethylene Oxide Segment. Raman data and XRD results[16] in our initial investigations indicated that 14−7−14 had a different $-(EO)_7-$ conformation compared to a sample crystallized from methanol. When 14−7−14 is crystallized from methanol, the layer spacing is 60.1 Å, while when it is crystallized from hexane, the spacing is shorter, giving a value of 52.7 Å. Evidently, the sample generated from methanol has a more extended PEO core, which is consistent with the Raman result.

Raman results show that 14−7−14 crystallized from hexane adopts a helical conformation, while that generated from methanol shows three bands that are characteristic of the planar zigzag conformation. The different solubility of PE and PEO units in a hydrophilic or hydrophobic solvent could explain the observation described above. In a hydrophilic solvent like methanol, the ethylene segments in 14−7−14 are less soluble and therefore crystallize first with a planar zigzag conformation. Then as the PEO cores crystallize, they adopt a trans conformation in order to conform to the predefined crystalline packing and trans structure defined by the ethylene segments. On the other hand, in a hydrophobic solvent like hexane, PEO cores are less soluble and therefore crystallize first with a helical conformation. When PE segments crystallize, they tilt

Table 3. Raman Bands in the Region 600−1800 cm^{-1} for Microblock Copolymers P(20, 7) and P(20,10)[a]

P(20,7) Raman shift (cm^{-1})	P(20,10) Raman shift (cm^{-1})	peak assignment	contribution	conformation
842 w	839 s	$r(CH_2)$	helical	tgt
1037 w			planar zigzag	ttt
1061 s	1062 m	$r(CH_2)$, $\nu_s(COC)$		tgt, ttt
1126 s	1128 m	$\nu_s(COC)$		ttt, tgt
1148 s			planar zigzag	ttt
	1237 w	$t(CH_2)$	helical	ttt, ttg, tgt
1245 w				
1274 m	1280 m	$t(CH_2)$		ttt, tgt
1295 s	1295 s			
1440 s	1439 s	$\delta(CH_2)$		tgg, tgt
	1481 m	$\delta(CH_2)$	helical	tgt
1495 s			planar zigzag	ttt

[a] Band intensities: w (weak); m (medium); s (strong). Mode: r (rocking); t (torsion); ν (stretching); δ (bending). The assignment subscripts "a" and "s" stand for asymmetric and symmetric motions.

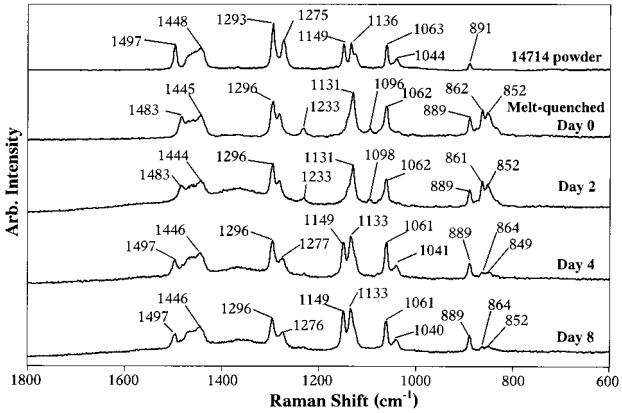

Figure 4. Conformational transition of $(EO)_7$ in $E_{14}-(EO)_7-E_{14}$ by melt-quenching and annealing. The planar zigzag conformation of $-(EO)_7-$ sequence changes to a helical one immediately upon melt-quenching. However, annealing at room temperature for several days produces a gradual return to the planar zigzag conformation.

with respect to the axis of the helical core to increase packing density.

Conclusions

Raman spectroscopy has indicated that the conformation of a $(CH_2CH_2O)_n$ block can be affected by many factors such as mechanical stretching, molecular architecture, thermal history, and solvent. A metastable planar zigzag $(EO)_n$ conformation was observed in mechanically stretched PEO samples held under tension. Interestingly enough, this conformation becomes stable when the ethylene oxide block is chemically constrained by adjacent crystalline blocks, such as in triblocks or microblock copolymers.

We investigated the behavior of a series of $14-n-14$ triblocks by varying n from 3 to14. Spectroscopic results showed that there are conformational variations within the series, and the conformation of the $-(EO)_n-$ cores is dependent on the core length. The magic number 7, the length of the $-(EO)_n-$ core, is critical in determining the helical−planar zigzag transition for triblock oligomers with ABA architecture. Of significant interest is that the conformational variations observed, for the EO sequence in the triblock, also appears in their high molecular weight copolymer, P(20,n) with n varying from 7 to 14.

Experimental results not only demonstrated that 14−7−14 exhibits different conformations upon melt-quenching but that this process is reversible upon annealing at room temperature for several days. Finally, we obtained either a helical or planar zigzag conformation for the $-(EO)_7-$ of a triblock, 14−7−14, in different solvents.

The structural variations observed above will be used to choose a second series of triblocks for investigation in which n is constant and m varies from 6 to 16. In this way, we will be able to construct an intramolecular "phase diagram" as a function of triblock composition. The same method could be applied to their microblock copolymer counterparts; that is, we could also construct a map of ethylene oxide and ethylene conformational structure as a function of microblock copolymer composition. This result would allow useful prediction of structure−property relationships in microblock copolymers and provide a correlation between copolymer properties (thermal, structural, mechanical, etc.) and the composition (m vs n) of the copolymer repeat unit, $-[E_m-(EO)_n]-$.

Acknowledgment. J.F.R. acknowledges several helpful discussions with Dr. Andy Lovinger, NSF, concerning the crystallization of ethylene oxide sequences. The Raman instrumentation used in these studies was obtained with partial assistance from the NSF Instrumentation for Materials Research Program (DMR-9704127) and an Army Grant (DURIP DAAG55-97-1-0081). J.F.R. also acknowledges the NSF (DMR-9812088) and DOE PAIR Program for partial support during the course of this work.

References and Notes

(1) Bates, F. S.; Fredrickson, G. H. *Annu. Rev. Phys. Chem.* **1990**, *41*, 525.
(2) Hamley, I. W. *The Physics of Block Copolymers;* Oxford, University Press: New York, 1998.
(3) Chen, W. Y.; Alexandridis, P.; Su, C. K.; Patrickios, C. S.; Hertler, W. R.; Hatton, T. A. *Macromolecules* **1995**, *28*, 8604.
(4) Patrickios, C. S.; Lowe, A. B.; Armes, S.; Billingham, N. C. *J. Polym. Sci., Polym. Chem. Ed.* **1998**, *36*, 617.
(5) Yu, G.; Eisenberg, A. *Macromolecules* **1998**, *31*, 55.
(6) Mao, G.; Clingman, S. R.; Ober, C. K.; Long, T. E., *Polym. Prepr. (Am. Chem. Soc., Div. Polym. Chem.)* **1993**, *34* (2), 710.
(7) Twieg, R.; Rabolt, J. F. *J. Polym. Sci., Polym. Lett. Ed.* **1983**, *21*, 901.
(8) Rabolt, J. F.; Russell, T. P.; Twieg, R. *Macromolecules* **1984**, *17*, 2786.
(9) Russell, T. P.; Twieg, R.; Farmer, B. L.; Siemens, R.; Rabolt, J. F. *Macromolecules* **1986**, *19*, 1135.
(10) Davidson, T.; Griffin, A. C.; Wilson, L. M.; Windle, A. H. *Macromolecules* **1995**, *28*, 354.

(11) Tashiro, K.; Tadokoro, H. *Rep. Prog. Poly. Phys. Jpn.* **1978**, *21*, 417.
(12) Tadokoro, H.; Chatani, Y.; Yoshihara, T.; Tahara, S.; Murahashi, S. *Macromol. Chem.* **1964**, *73*, 109.
(13) Takahashi, Y.; Sumita, I.; Tadokoro, H. *J. Polym. Sci., Polym. Phys. Ed.* **1973**, *11*, 2115.
(14) Maxfield, J.; Shepherd, I. W. *Polymer* **1975**, *16*, 506.
(15) Yoshihara, T.; Tadokoro, H.; Murahashi, S. J. *Chem. Phys.* **1964**, *41*, 2902.
(16) Chen, Y.; Baker; G. L.; Ding, Y.; Rabolt, J. F. *J. Am. Chem. Soc.* **1999**, *121*, 6963.
(17) Frech, R.; Chintapalli, S.; Bruce, P. G.; Vincent, C. A. *Macromolecules* **1999**, *32*, 808.
(18) Chen, Y.; Baker, G. L. *J. Org. Chem.* **1999**, *64*, 6870.
(19) Qiao, J.; Chen, Y.; Baker, G. L. *Chem. Mater.* **1999**, *11*, 2542.

MA011511O